

Initial Clinical Results of a Novel Immuno-PET Theranostic Probe in HER2-negative Breast Cancer

Caroline Rousseau^{1,2}, David M. Goldenberg^{3,4}, Mathilde Colombié¹, Jean-Charles Sébille¹, Philippe Meingan⁵, Ludovic Ferrer^{2,6}, Pierre Baumgartner⁷, Evelyne Cerato⁸, Damien Masson⁹, Mario Campone¹⁰, Aurore Rauscher⁷, Vincent Fleury¹, Catherine Labbe⁵, Alain Faivre Chauvet¹¹, Jean-Sebastien Fresnel¹⁰, Claire Toquet¹², Jacques Barbet¹³, Robert M. Sharkey³, Loic Champion^{2,14}, Françoise Kraeber-Bodéré^{1,2,11}

1 Nuclear Medicine, ICO Cancer Center, Nantes, FRANCE

2 CRCINA, University of Nantes and Angers, INSERM UMR1232, CNRS-ERL6001.

3 Immunomedics, Inc., Morris Plains, NJ, USA

4 IBC Pharmaceuticals, Inc., Morris Plains, NJ, USA

5 Radiology, ICO Cancer Center, Nantes, FRANCE

6 Physics, ICO Cancer Center, Nantes, FRANCE

7 Pharmacy, ICO Cancer Center, Nantes, FRANCE

8 DRCl, University Hospital, Nantes, FRANCE

9 Biology Department, University Hospital, Nantes, FRANCE

10 Oncology, ICO Cancer Center, Nantes, FRANCE

11 Nuclear Medicine, University Hospital, Nantes, FRANCE

12 Pathology Department, University Hospital, Nantes, FRANCE

13 GIP Arronax, Saint-Herblain, FRANCE

14 Biometrics, ICO Cancer Center, Nantes, FRANCE

Corresponding author: Caroline Rousseau, MD, PhD, ICO Gauducheau Cancer Center, Boulevard Monod, 44805 Saint Herblain Cedex; e-mail : c-rousseau@ico.unicancer.fr.

Keywords: Breast cancer, Immuno-PET, pretargeting, bispecific antibody, gallium-68

Running Title: Pretargeted immuno-PET in breast cancer

Support: Supported in part by grants from the University Hospital of Nantes and Fondation Avenir in 2010, the French National Agency for Research, called “Investissements d’Avenir” IRON Labex ANR-11-LABX-0018-01 and ArronaxPlus Equipex ANR-11-EQPX-0004 and by a grant INCa-DGOS-Inserm_12558 (SIRIC ILIAD).

Prior Presentation: Presented in part at the 2014 European Nuclear Medicine Congress in Göteborg, Sweden, at the 2014 San Antonio Breast Cancer Symposium in San Antonio, Texas, and at the 2015 Annual Meeting of the American Society of Clinical Oncology in Chicago, Illinois.

ACKNOWLEDGEMENTS: We thank the patients and their families for their participation, and S Belcheva and the nuclear medicine technologists at the ICO Cancer Center for their contributions.

ABSTRACT

Purpose

This prospective study evaluated the imaging performance of a novel immunological pretargeting positron-emission tomography (immuno-PET) method in patients with HER2-negative, carcinoembryonic antigen (CEA)-positive, metastatic breast cancer (BC), compared to computed tomography (CT), bone magnetic resonance imaging (MRI), and ¹⁸fluorodeoxyglucose PET (FDG-PET).

Patients and Methods

Twenty-three patients underwent whole-body immuno-PET after injection of 150 MBq ⁶⁸Ga-IMP288, a histamine-succinyl-glycine peptide given following initial targeting of a trivalent anti-CEA, bispecific, anti-peptide antibody. The gold standards were histology and imaging follow-up. Tumor standard uptake values (SUV_{max} and SUV_{mean}) were measured, and tumor burden analyzed using Total Tumor Volume (TTV) and Total Lesion Activity (TLA).

Results

Total lesion sensitivity of immuno-PET and FDG-PET were 94.7% (1116/1178) and 89.6% (1056/1178), respectively. Immuno-PET had a somewhat higher sensitivity than CT and FDG-PET in lymph nodes (92.4% vs 69.7% and 89.4%, respectively) and liver metastases (97.3% vs 92.1% and 94.8%, respectively), whereas sensitivity was lower for lung metastases (48.3% vs 100% and 75.9%, respectively). Immuno-PET showed higher sensitivity than MRI and FDG-PET for bone lesions (95.8% vs 90.7% and 89.3%,

respectively). In contrast to FDG-PET, immuno-PET disclosed brain metastases. Despite equivalent tumor SUV_{max} , SUV_{mean} , and TTV, TLA was significantly higher with immuno-PET compared to FDG PET ($P=0.009$).

Conclusion

Immuno-PET using anti-CEA/anti-IMP288 bispecific antibody, followed by ^{68}Ga -IMP288, is a potentially sensitive theranostic imaging method for HER2-negative, CEA-positive, metastatic BC patients, and warrants further research.

INTRODUCTION

Breast cancer (BC) is the most common cancer among women worldwide, and about 40% of all BC patients suffer a recurrence (1). Imaging plays an important role in BC management, and positron-emission tomography using ^{18}F fluorodeoxyglucose (FDG-PET) is recommended for relapse detection and therapy assessment (2). However, FDG is not an oncological-specific tracer, and doesn't allow selection of patient for hormonal or targeted therapies. Recently, ^{18}F fluoro-estradiol was approved for the characterization of estrogen receptor expression in known or suspected metastatic lesions of ER-positive BC (3).

In the last decade, a promising option to improve diagnostic and theranostic imaging has been immuno-PET, which combines the high sensitivity and quantitative capabilities of PET with the specificity and selectivity of a monoclonal antibody (MAb) against a given tumor cell-surface marker. This combination potentially provides a noninvasive, *in vivo* quantifiable, three-dimensional whole-body tumor biomarker expression cartography, permitting tumor detection and patient monitoring prospectively (4). In BC, clinical studies have reported a good performance of immunoconjugates targeting HER2 radiolabeled with PET emitters having different half-lives (^{68}Ga , ^{64}Cu and ^{89}Zr) (5,6), and in preclinical studies, several biomarkers, such as syndecan-1, have been considered for triple-negative BC (7,8).

Carcinoembryonic antigen (CEA), specifically carcinoembryonic antigen cell-adhesion molecule-5 (CEACAM5), represents an attractive target in BC, with serum CEA positivity (i.e., ≥ 5 ug/L) being observed in 50% to 60% of patients with metastatic disease (9), with

a false-positive result of 5% (10). A recent meta-analysis showed that elevated CEA was significantly associated with poorer disease-free survival and overall survival in BC, independent of tumor size, lymph node metastasis, or tumor grade and irrespective of ER or HER2 status (11,12). Elevated CEA was more related to the non-triple-negative and non-luminal tumor type and older age (12). Moreover, the majority of invasive lobular, tubular, and cribriform carcinomas were CEA-negative (72%). Conversely, 70% of invasive ductal carcinomas were CEA-positive (13).

In the 1970's and later, the potential of cancer imaging using ^{131}I - and $^{99\text{m}}\text{Tc}$ -labelled anti-CEA antibodies was reported in CEA-positive tumors, including BC, but the method was limited by the poor resolution of single-photon emission computed tomography (SPECT) and the high blood activity observed with directly-radiolabeled MAbs and fragments (14-17). Anti-CEA targeted therapies are still under development, and labetuzumab govitecan (anti-CEACAM5/SN-38 antibody-drug conjugate) recently has shown promising efficacy with manageable toxicity in metastatic colorectal cancer patients (18). Durable objective responses in highly pretreated metastatic triple-negative BC patients, as well as in ER-positive, HER2-negative BC, were reported with an antibody–drug conjugate that targets the human trophoblast cell-surface antigen-2 (TROP-2), suggesting the advance of a targeted drug–conjugate platform for solid tumors (19,20).

Pretargeting refers to a system of improved image contrast and high sensitivity obtained by first administering an anti-CEA bispecific antibody (BsMAb), followed by haptens labeled with ^{111}In or ^{131}I (21-23). TF2 is an engineered trivalent BsMAb composed of a humanized anti–histamine-succinyl-glycine Fab fragment derived from the murine 679 antibody and 2 humanized anti-CEA Fab fragments (trivalency) of the humanized hMN-

14 antibody, formed into a 157-kD protein by the “Dock-and-Lock” procedure (24). The ^{68}Ga -IMP288 bivalent peptide pretargeted with TF2 has demonstrated promising immuno-PET performance in a pilot optimization clinical trial (25). The current prospective study was designed to assess the initial sensitivity, safety, and preferred conditions of pretargeting immuno-PET using the BsMAb TF2 and the ^{68}Ga -IMP288 peptide, in comparison to FDG-PET and conventional imaging in relapsed, HER2-negative, BC patients.

PATIENTS AND METHODS

Population

Patients ≥ 18 years, with progressive HER2-negative metastatic BC, after standard treatments and presenting with a CEA serum level ≥ 10 ng/ml, and with at least one lesion ≥ 10 mm on conventional imaging (CT, MRI, and bone scan), were eligible. The other inclusion criteria were Karnofsky performance status ≥ 70 , minimum life expectancy of 6 months, creatinine ≤ 2.5 x normal, normal serum human anti-mouse antibody and human anti-human antibody (HAHA) titers. Women of child-bearing potential must have a negative pregnancy test. The exclusion criteria were pregnancy and breast feeding, any serious active disease or co-morbid medical condition, any history of another cancer during the last 5 years, with the exception of non-melanoma skin tumors or stage 0 (*in-situ*) cervical carcinoma, and a known hypersensitivity to antibodies or proteins. In the 4 weeks preceding immuno-PET, a staging workup that included a complete history, physical examination, CEA and CA15-3 serum level measurements (with biomarker doubling time determination when possible) were performed. The patients underwent morphological imaging (thoracic-abdominal-pelvic contrast-enhanced CT for extra-bone lesion evaluation and pelvic-spine MRI for bone evaluation), and also FDG-PET. The trial sponsored by Nantes University Hospital was approved by the responsible ethics committee (CPP), and registered at ClinicalTrials.gov (NCT01730612) and all patients signed written informed consent. Enrollment was at the ICO Cancer Center associated with Nantes University Hospital of the GCS IRCNA.

Investigational products and study design

The reagents were prepared for human use by Immunomedics, Inc. (Morris Plains, NJ, USA), whereby sufficient quantity was produced to complete a small feasibility and safety study. A 1.85-GBq (at calibration time) pharmaceutical-grade gallium-68 generator (Eckert-Ziegler, Germany) was used. ^{68}Ga -IMP288 was obtained with a specific activity of 40 to 100 MBq/nmol, with a radiochemical purity > 95%.

TF2 diluted in 250 mL 0.9% NaCl and ^{68}Ga -IMP288 in 50 mL of 0.9% NaCl were administered by I.V. infusion over 30 minutes. Patients were premedicated with oral anti-histamine the day before TF2 infusion and with I.V. 5 mg anti-histamine (polaramine) and 500 mg corticosteroid (hydrocortisone hemisuccinate) 5 minutes before infusion of 60 to 120 nmol of TF2, and 3 to 6 nmol of ^{68}Ga -IMP288 administered 24 to 30 h later. Four different conditions of pretargeting (molar doses of BsMAb and peptide and delay) were assessed for pharmacokinetics optimization purposes. Because there was no statistically-significant differences between the cohorts, the results of the 4 cohorts were combined to compare sensitivity of immuno-PET with FDG-PET or conventional imaging.

Safety was assessed by monitoring vital signs, physical examination, and adverse events. HAHA titers were determined by Immunomedics (Morris Plain, New Jersey) at 3 and/or 6 months, and up to 9 months in some cases, using an ELISA method (abnormal when \geq 50 ng/mL) (25).

Immuno-PET imaging

PET/CT was performed using a 4-ring Siemens Biograph mCT system with time of flight capability 60 and 120 minutes after injection of 150 MBq of ^{68}Ga -IMP288, and

reconstructed using a 3D ordinary Poisson-OSEM with point-spread function correction and TOF mode (3 iterations, 21 subsets, 2-mm full width at half maximum Gaussian post-filtering, voxel size: 4'4'2 mm³). Whole-body acquisitions were performed under spontaneous breathing for 2.5 min per bed position. CT was obtained using variable mAs, 120 kVp and a pitch of 1 without contrast enhancement. Acquisitions were performed from the top of the head to mid-thigh (6 to 8 steps per patient).

Qualitative Imaging Analysis

Immuno-PET abnormal uptake was defined visually as focal increase of uptake higher than the surrounding background. For skeletal and liver lesions, if more than 10 lesions per bone and similarly for the entire liver were counted, the lesion number was nevertheless capped at ten. Blinded to the other diagnostic results, CT and bone MRI were analyzed by consensus of two radiologists (CL, PM) with expertise in oncology, and FDG-PET and immuno-PET by consensus of two nuclear medicine physicians (FKB, CR) with expertise in immunotargeting and PET. For both ethical and practical reasons, not every suspected lesion was evaluated by histology. Complementary imaging, primarily MRI, was performed to assess the most important lesions suspected by immuno-PET and not detected by the initial work-up (CT and bone MRI). The gold standard was therefore determined on the basis of histology and imaging follow-up. Indeed, FDG-PET, CT, pelvic-spinal MRI, and any added imaging were performed 3 months after immuno-PET to confirm the abnormalities.

True-positive (TP) results corresponded to an abnormal image by an imaging method and confirmed by histology or detected by at least one other imaging modality and confirmed by follow-up. A negative finding on an imaging method was considered to be false-

negative (FN) if positive by one other imaging method plus histopathology, or by one other imaging method and confirmed by follow-up. Percent sensitivity $[(TP/TP + FN) \times 100]$ on a lesion basis was calculated for each imaging modality.

Semi-quantitative immuno-PET and FDG-PET analyses

With a threshold of 40%, maximum and mean tumor standard uptake values (Tumor SUV_{max} and SUV_{mean}) were measured on tumor foci for immuno-PET and FDG-PET and the partial volume effect was corrected. Analysis of tumor burden was performed using Total Tumor Volume (TTV, the sum in cubic centimeters of the tumor volume of each single positive lesion), and Total Lesion Activity (TLA, tumor volume x SUV_{mean}) obtained automatically with Oncoplanet software (version 2.0 RC, Dosisoft).

Statistical Analysis

The continuous variables (Tumor SUV_{max}, Tumor SUV_{mean}, TTV, and TLA) were described by median and interquartile range (IQR). Variable comparisons between FDG-PET and Immuno-PET were performed by means of the Wilcoxon signed-rank test. All comparisons were two-sided, with a significance limit < 5%. All calculations were made using the Stata SE 13.1 statistical tool (StataCorp LP, College Station, Texas 77845, USA).

RESULTS

Patient characteristics and adverse events

The demographics of the 23 metastatic HER2-negative BC patients, all women, are presented in Table 1. Two patients benefited from a second immuno-PET coupled with a second FDG-PET, accounting for 25 immuno-PET and FDG-PET studies in the 23 patients.

No patient experienced an anaphylactic reaction during or after the TF2 BsMAb or hapten infusions. HAHA levels were abnormal in 4/25 (16%) patients, but normalized within nine months.

Imaging results and sensitivity

As shown in a previous study with the same radiopharmaceutical (25), the physiological distribution of the tracer showed moderate liver and spleen uptake, renal elimination, and presence in the heart and blood vessels due to the circulation of the radiopharmaceutical.

A total of 1,178 lesions were confirmed according the gold standard: 66 in lymph nodes, 29 in the lungs, 153 in the liver, 919 in bone/bone marrow, and 11 in other sites (1 cutaneous, 3 adrenal, 1 ovarian, 1 mammary, and 5 cerebral). All patients had evidence of metastatic disease on immuno-PET, FDG-PET, CT, and bone MRI (Table 2).

A total of 1,116 foci were detected by immuno-PET, all confirmed as TP according to the gold standard, and 62 lesions were missed (FN lesions), predominantly in lung and bone. All immuno-PET lesions were seen at 60 as well as 120 minutes. FDG-PET, CT, and bone MRI detected 1,056, 216, and 412 TP lesions, respectively, and presented 122, 35, and

42 FN results, respectively (Table 2). The mammary and cutaneous sites were detected by CT, FDG-PET and immuno-PET, whereas CT missed the adrenal lesions and FDG-PET missed the ovarian lesion. Interestingly, immuno-PET detected 5 brain lesions confirmed by brain MRI, whereas brain imaging was difficult by FDG-PET (4 FN), because of physiological cerebral FDG uptake (Figure 1).

Immuno-PET showed a somewhat higher overall sensitivity (94.7%) than FDG-PET (89.6%). Regarding the different metastatic sites, immuno-PET also had a higher sensitivity than CT and FDG-PET for lymph node (92.4% vs 69.7% and 89.4%, respectively) and liver (97.3% vs 92.1% and 94.8%, respectively), whereas sensitivity was lower for lung metastases (48.3% vs 100% and 75.9%, respectively). Immuno-PET had a slightly higher sensitivity for bone evaluation than MRI and FDG-PET (95.8% vs 90.7% and 89.3%, respectively) (Figure 2).

The median size of liver, lung, and lymph node lesions were 24 mm [range 10-103 mm], 10.5 mm [range 6-19 mm], and 28 mm [range 9-43 mm], respectively. Of all the lesions identified by FDG and immuno-PET, three (a lymph node, bone, and a cutaneous lesion) were evaluated by IHC. Diffuse and heterogenous staining (1+ to 3+ intensity) was seen in over 50% of the carcinoma cells (example of lymph node staining shown in Figure 3).

PET quantitative metrics

For determination of immuno-PET SUV, TTV, and TLA, only the 15 patients injected with optimized pretargeting parameters according Bodet-Milin's study were considered because these cohorts represent optimal pretargeting conditions that would be used if the technique was in clinical practice (i.e., a BsMAB-to-peptide mole ratio of 20 or 40 and a 30

h pretargeting delay) (21). Tumor uptake was not significantly different between immuno-PET and FDG-PET, with a median SUV_{max} of 23.83 [IQR: 9.09-44.65] and 15.87 [IQR: 11.70-18.87], respectively ($P=0.088$), and a median SUV_{mean} of 4.90 [IQR: 3.00-8.16] and 4.71 [IQR: 3.49-5.62], respectively ($P=0.125$) (Table 3). Tumor burden evaluated by functional volumes was equivalent between both PET methods, with median TTV equal to 294 [IQR: 159-558] for immuno-PET and 299 [IQR: 139-410] for FDG-PET ($P=0.256$), whereas tumor activity TLA was significantly higher with immuno-PET (median of 2,123; IQR: 995-5,304) compared to FDG-PET (median of 1,197; IQR: 355-2,433; $P=0.009$). When considering the entire patient population, as described in Figure 4, a correlation was found between the SUV_{max} of the most intense lesion in immuno-PET and the serum CEA level ($P = 0.0396$), whereas no correlation was found between FDG-PET tumor SUV_{max} and the CEA serum level.

DISCUSSION

CEA represents a potential target for antibody-based imaging or therapy in several solid tumors, including ER-positive, HER2-negative, and triple-negative BC (14-18, 26). Moreover, the discrepancy between serum CEA levels and CEA tissue expression in patients with breast cancer is well-known. Whereas immunohistochemistry (IHC) shows positive CEA expression in 70-90%, serum CEA levels are often within the normal range (16). Further, IHC is often performed only on a tumor biopsy (i.e., a small fragment of the disease), an anti-CEA PET imaging study will allow an evaluation of CEA expression in tumors disseminated throughout the whole body. Indeed, it is possible that an examination of the heterogeneity of CEA expression in the disseminated tumors, as elucidated by imaging, may improve the prediction for anti-tumor responses. This initial study is the first demonstrating the excellent sensitivity of anti-CEA pretargeted immuno-PET in HER2-negative, metastatic BC, suggesting its potential for tumor imaging or theranostic approaches in this subtype of BC or other CEA-expressing tumors.

In this study, pretargeted immuno-PET achieved a 94.7% overall sensitivity, with a somewhat better sensitivity than morphological imaging and FDG-PET for lymph node, liver, and bone examinations in BC patients with metastatic disease. As described in the literature, the number of FN results by FDG-PET may be accentuated by the majority of patients having a hormonal status of ER+ and/or PR+ (2). However, in contrast to FDG-PET, immuno-PET detected brain metastases, potentially providing improved patient management due to the possibility of theranostic targeting of cerebral dissemination. Disappointingly, immuno-PET was less effective than CT and FDG-PET for lung metastasis detection, where the sensitivity of CT and FDG-PET were consistent with those reported previously (27,28). ^{68}Ga -PET has a larger range than ^{18}F (6.10 vs 0.54 mm in

lung tissue, respectively), reducing PET image resolution, while the spontaneous breathing PET-CT acquisition associated with a partial volume may affect PET performance with ^{68}Ga more than ^{18}F for detection of small lung lesions (median value of 10.5 mm in this cohort) (29). Moreover, Laessing et al. reported a lower expression of CEA in lung metastases, compared to liver and bone metastases (30), which may explain the poorer performance of immuno-PET in this region. However, labeling of the peptide with ^{18}F , as described previously, may improve the detection of small lung lesions (31) without altering radiation exposure, since Ga-68 and F-18 have similar exposure rates ($1.79 \cdot 10^{-4} \text{ mSv} \cdot \text{m}^2 \cdot \text{MBq}^{-1} \cdot \text{h}^{-1}$ for Ga-68 and $1.87 \cdot 10^{-4} \text{ mSv} \cdot \text{m}^2 \cdot \text{MBq}^{-1} \cdot \text{h}^{-1}$ for F-18).

CEA, especially CEACAM5, functions as a cell-adhesion molecule during tumor invasion of the lymphatic lumen, possibly explaining the high sensitivity for lymph node detection (32). Indeed, immunohistochemistry confirmed a strong cellular CEA expression in a lymph node showing high uptake in one case. Finally, even if imaging specificity requiring histological confirmation of false-positive lesions was not determined in this cohort of patients with diffuse disease, immuno-PET is expected to have a higher specificity than FDG-PET. This needs further study.

Despite the absence of a significant difference between immuno-PET and FDG-PET for tumor SUV_{max} and SUV_{mean} , which reflect the activity of the most intense lesion, the TLA, reflecting tumor volume and uptake intensity of all whole-body foci, was significantly higher for immuno-PET than FDG-PET. The TTV, being comparable for the two PET methods, suggests that using CEA-targeting will result in a higher tumor intensity with whole-body imaging, compared to utilizing a glucose metabolism tracer, such as with FDG-PET.

This initial study also confirmed that intravenous injections of corticosteroids and anti-histamines before TF2 and IMP-288 peptide infusions may induce transient

immunodepression, limiting immediate and delayed immune reactions. The 16% HAHA response rate resolved at 9 months in all cases, and was similar to those reported by Bodet-Milin et al. previously, and lower than those reported by Schoffelen et al. (52%) (25,33).

Finally, immuno-PET with the two-step pretargeting method described herein enables the use of short half-life PET emitters, such as ^{68}Ga or ^{18}F , allowing image acquisition only a few hours after peptide injection, whereas using an intact IgG instead of a Fab fragment requires imaging a few days after the MAb injection for optimal contrast (due to the delayed immunoglobulin tumor targeting and clearance from the circulation). Intact IgG requires radiolabeling with long half-life radionuclides, such as ^{89}Zr or ^{124}I , which are less favorable in terms of dosimetry. However, pretargeting approaches require optimization studies to determine the best BsMAb and peptide molar dose ratio and pretargeting delay. The TF2/ ^{68}Ga -IMP288 system used here has already been evaluated in a study of medullary thyroid cancer patients, concluding that a 120-nmol BsMAb dose, a molar ratio of 20, and a 30-h pretargeting delay represent optimal conditions (25). The present study in BC patients confirmed the higher tumor uptake and contrast using 120 nmol of BsMAb and a 30-h pretargeting delay, compared to a 60-nmol BsMAb dose or a 24-h pretargeting delay (Supplemental Table 1), but this requires confirmation in a larger study.

In conclusion, this initial feasibility study demonstrated that anti-CEA immuno-PET using a pretargeted trivalent, bispecific antibody and then a ^{68}Ga -IMP288 small peptide is a feasible and safe procedure for detecting metastatic lesions in HER2-negative, metastatic, BC patients. Immuno-PET targeting CEA showed a higher overall sensitivity than FDG-PET for disclosing metastases, including dissemination in the brain, and thus offers the

possibility of an *in-vivo* evaluation of CEA-expression and disclosure of whole-body tumor burden, including lesions not accessible to biopsy. Immuno-PET is a potential theranostic molecular imaging technique to select patients for an antibody-based individualized therapy because of metastatic tumor heterogeneity and the discrepancy between serum levels and tissue expression of the antigen in patients.

DISCLOSURES

DMG and RMS own Immunomedics stock or stock options, and Dr. Goldenberg has royalty-bearing patented inventions. Dr. Goldenberg is the founder and retired Chief Scientific Officer of Immunomedics, Inc., and the founder and retired Chairman of IBC Pharmaceuticals, Inc. Dr. Sharkey is a consultant to Immunomedics, Inc.

No other potential conflicts of interest relevant to this article were reported.

The proprietary TF2 and IMP288 reagents were provided by Immunomedics, Inc., and IBC Pharmaceuticals, Inc..

KEY POINTS

QUESTION: Is anti-CEA pretargeting immuno-PET using the BsMAb TF2 and the 68Ga-IMP288 peptide a potential theranostic molecular imaging technique to select HER2-negative BC patients for an antibody-based individualized therapy ?

PERTINENT FINDINGS: In a prospective clinical trial comparing sensitivity of anti-CEA pretargeting immuno-PET to FDG-PET for 23 HER2-negative metastatic BC patients, we showed a higher overall sensitivity of immuno-PET (94.7%) than FDG-PET (89.6%) for disclosing metastases, in particular in brain, and thus offers the possibility of an *in-vivo* evaluation of CEA-tumor expression, including lesions not accessible to biopsy.

IMPLICATIONS FOR PATIENT CARE: Anti-CEA pretargeting immuno-PET appears to be an efficient theranostic molecular imaging technique for an antibody-based individualized therapy to select patients unable to receive trastuzumab.

REFERENCES

1. Gerber B, Freund M, Reimer T. Recurrent breast cancer: treatment strategies for maintaining and prolonging good quality of life. National Comprehensive Cancer Network. NCCN clinical practice guidelines in oncology. *Breast Cancer*. 2016;107:85-91.
2. Salaün PY, Abgral R, Malard O, et al. Good clinical practice recommendations for the use of PET/CT in oncology. *Eur J Nucl Med Mol Imaging*. 2019 Oct 21. doi: 10.1007/s00259-019-04553-8. [Epub ahead of print].
3. Peterson LM, Kurland BF, Schubert EK, et al. A phase 2 study of 16α -[^{18}F]-fluoro- 17β -estradiol positron emission tomography (FES-PET) as a marker of hormone sensitivity in metastatic breast cancer (MBC). *Mol Imaging Biol*. 2014;16:431-440.
4. de Lucas AG, Schuhmacher AJ, Oteo M, et al. Targeting MT1-MMP as an ImmunoPET-Based Strategy for Imaging Gliomas. *PLoS One*. 2016 27;11:e0158634.
5. Jauw YW, Menke-van der Houven van Oordt CW, Hoekstra OS, et al. Immuno-positron emission tomography with Zirconium-89-labeled monoclonal antibodies in oncology: what can we learn from initial clinical trials? *Front Pharmacol*. 2016;7:131.
6. Ulaner GA, Lyashchenko SK, Riedl C, et al. First-in-human human epidermal growth factor receptor 2-targeted imaging using ^{89}Zr -Pertuzumab PET/CT: dosimetry and clinical application in patients with breast cancer. *J Nucl Med*. 2018;59:900-906.

7. Rousseau C, Ruellan AL, Bernardeau K, et al. Syndecan-1 antigen, a promising new target for triple-negative breast cancer immuno-PET and radioimmunotherapy. A preclinical study on MDA-MB-468 xenograft tumors. *EJNMMI Res.* 2011;1:20.
8. Terwisscha van Scheltinga AG, Berghuis P, Nienhuis HH, et al. Visualising dual downregulation of insulin-like growth factor receptor-1 and vascular endothelial growth factor-A by heat shock protein 90 inhibition effect in triple negative breast cancer. *Eur J Cancer.* 2014;50:2508-2516.
9. Harris L, Fritsche H, Mennel R, et al. American Society of Clinical Oncology 2007 update of recommendations for the use of tumor markers in breast cancer. *J Clin Oncol.* 2007;25:5287-312.
10. Molina R, Barak V, van Dalen A, et al. Tumor markers in breast cancer- European Group on Tumor Markers recommendations. *Tumour Biol.* 2005;26:281-93.
11. Imamura M, Morimoto T, Nomura T, et al. Independent prognostic impact of preoperative serum carcinoembryonic antigen and cancer antigen 15-3 levels for early breast cancer subtypes. *World J Surg Oncol.* 2018;16:26.
12. Li X, Dai D, Chen B, Tang H, et al. Clinicopathological and prognostic significance of cancer antigen 15-3 and carcinoembryonic antigen in breast cancer: a meta-analysis including 12,993 patients. *Dis Markers.* 2018.2;2018:9863092.
13. Böcker W, Schweikhart G, Pollow K, et al. Immunohistochemical demonstration of carcinoembryonic antigen (CEA) in 120 mammary carcinomas and its correlation with tumor type, grading, staging plasma-CEA, and biochemical receptor status. *Pathol Res Pract.* 1985;180:490-7.

14. Goldenberg DM, DeLand F, Kim E, et al. Use of radiolabeled antibodies to carcinoembryonic antigen for the detection and localization of diverse cancers by external photoscanning. *N Engl J Med.* 1978; 22;298:1384-1386.
15. Goldenberg DM, Kim EE, De Land FH, et al. Radioimmunodetection of cancer with radioactive antibodies to carcinoembryonic antigen. *Cancer Res.* 1980;40:2984-2992.
16. Lind P, Smola MG, Lechner P, et al. The immunoscintigraphic use of Tc-99m-labelled monoclonal anti-CEA antibodies (BW 431/26) in patients with suspected primary, recurrent and metastatic breast cancer. *Int J Cancer.* 1991;47:865-9.
17. Goldenberg DM, Abdel-Nabi H, Sullivan CL, et al. Carcinoembryonic antigen immunoscintigraphy complements mammography in the diagnosis of breast carcinoma. *Cancer.* 2000;89:104-115.
18. Dotan E, Cohen SJ, Starodub AN, et al. Phase I/II trial of labetuzumab govitecan (anti-CEACAM5/SN-38 antibody-drug conjugate) in patients with refractory or relapsing metastatic colorectal cancer. *J Clin Oncol.* 2017;35:3338-3346.
19. Kalinsky K, Isakoff SJ, Tolaney SM, et al. Safety and efficacy of sacituzumab govitecan (anti-Trop-2-SN-38 antibody-drug conjugate) as ≥ 3 rd-line therapeutic option for treatment-refractory HER2-negative metastatic breast cancer (HER2Neg mBC). In: *San Antonio Breast Cancer Symposium*; Dec 4-8 2018; San Antonio, USA. Abstract P2-11-01.
20. Bardia A, Mayer IA, Vahdat LT, et al. Sacituzumab govitecan-hziy in refractory metastatic triple-negative breast cancer. *N Engl J Med.* 2019;380:741-751.

21. Peltier P, Curtet C, Chatal JF, et al. Radioimmunodetection of medullary thyroid cancer using a bispecific anti-CEA/anti-indium-DTPA antibody and an indium-111-labeled DTPA dimer. *J Nucl Med*. 1993;34:1267–1273.
22. Barbet J, Peltier P, Bardet S, et al. Radioimmunodetection of medullary thyroid carcinoma using indium-111 bivalent hapten and anti-CEA/anti-DTPA-indium bispecific antibody. *J Nucl Med*. 1998;39:1172–1178.
23. Oudoux A, Salaun P-Y, Bournaud C, et al. Sensitivity and prognostic value of positron emission tomography with F-18-fluorodeoxyglucose and sensitivity of immunoscintigraphy in patients with medullary thyroid carcinoma treated with anticarcinoembryonic antigen-targeted radioimmunotherapy. *J Clin Endocrinol Metab*. 2007;92:4590–4597.
24. Rossi EA, Goldenberg DM, Cardillo TM, et al. Stably tethered multifunctional structures of defined composition made by the dock and lock method for use in cancer targeting. *Proc Natl Acad Sci USA*. 2006;103:6841–6846.
25. Bodet-Milin C, Faivre-Chauvet A, Carlier T, et al. Immuno-PET using anticarcinoembryonic antigen bispecific antibody and ⁶⁸Ga-labeled peptide in metastatic medullary thyroid carcinoma: clinical optimization of the pretargeting parameters in a first-in-human trial. *J Nucl Med*. 2016;57:1505-1511.
26. Waaijer SJH, Warnders FJ, Stienen S, et al. Molecular imaging of radiolabeled bispecific T-cell engager ⁸⁹Zr-Amg211 targeting cea-positive tumors. *Clin Cancer Res*. 2018;24:4988-4996.
27. Yang HL, Liu T, Wang XM, et al. Diagnosis of bone metastases: a meta-analysis comparing ¹⁸F-FDG PET, CT, MRI and bone scintigraphy. *Eur Radiol*. 2011;21:2604–2617.

28. Piva R, Ticconi F, Ceriani V, et al. Comparative diagnostic accuracy of ¹⁸F-FDG PET/CT for breast cancer recurrence. *Breast Cancer*. 2017;9:461-471.
29. Sanchez-Crespo A. Comparison of Gallium-68 and Fluorine-18 imaging characteristics in positron emission tomography. *Appl Radiat Isot*. 2013;76:55-62.
30. Laessig D, Nagel D, Heinemann V, et al. Importance of CEA and CA15-3 during disease progression in metastatic breast cancer patients. *Anticancer Res*. 2007;27:1963-1968.
31. Schoffelen R, van der Graaf WT, Sharkey RM, et al. Pretargeted immuno-PET of CEA-expressing intraperitoneal human colonic tumor xenografts: a new sensitive detection method. *EJNMMI Res*. 2012;2:5.
32. Benchimol S, Fuks A, Jothy S, et al. Carcinoembryonic antigen, a human tumor marker, functions as an intercellular adhesion molecule. *Cell*. 1989;57:327-334.
33. Schoffelen R, Boerman OC, Goldenberg DM, et al. Development of an imaging-guided CEA-pretargeted radionuclide treatment of advanced colorectal cancer: First clinical results. *Br J Cancer*. 2013;109:934-942.

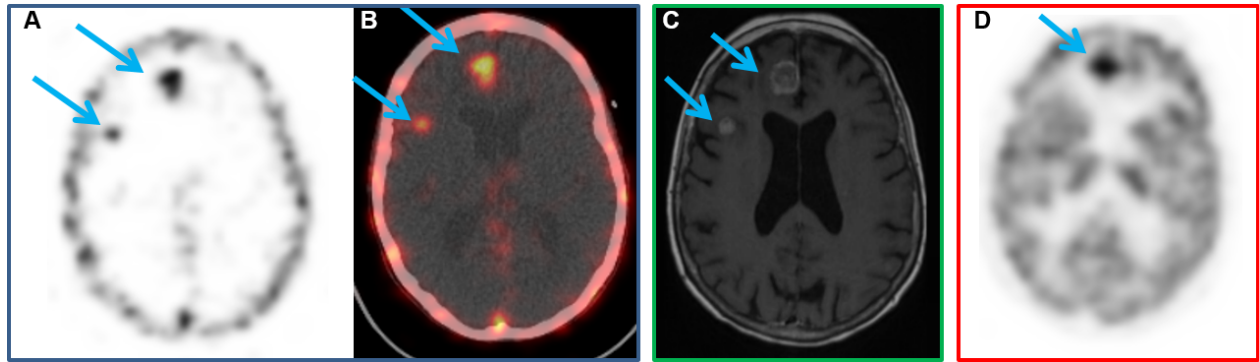


Figure 1: (A and B) Pretargeted immuno-PET with TF2 and ⁶⁸Ga-IMP288 peptide reveals two unknown brain metastases (right frontal and right fronto-parietal, blue arrows). (C) T1 Gadolinium MRI brain image confirms both asymptomatic lesions (blue arrows). (D) FDG-PET image shows only one metastasis (right frontal lesion, blue arrow).

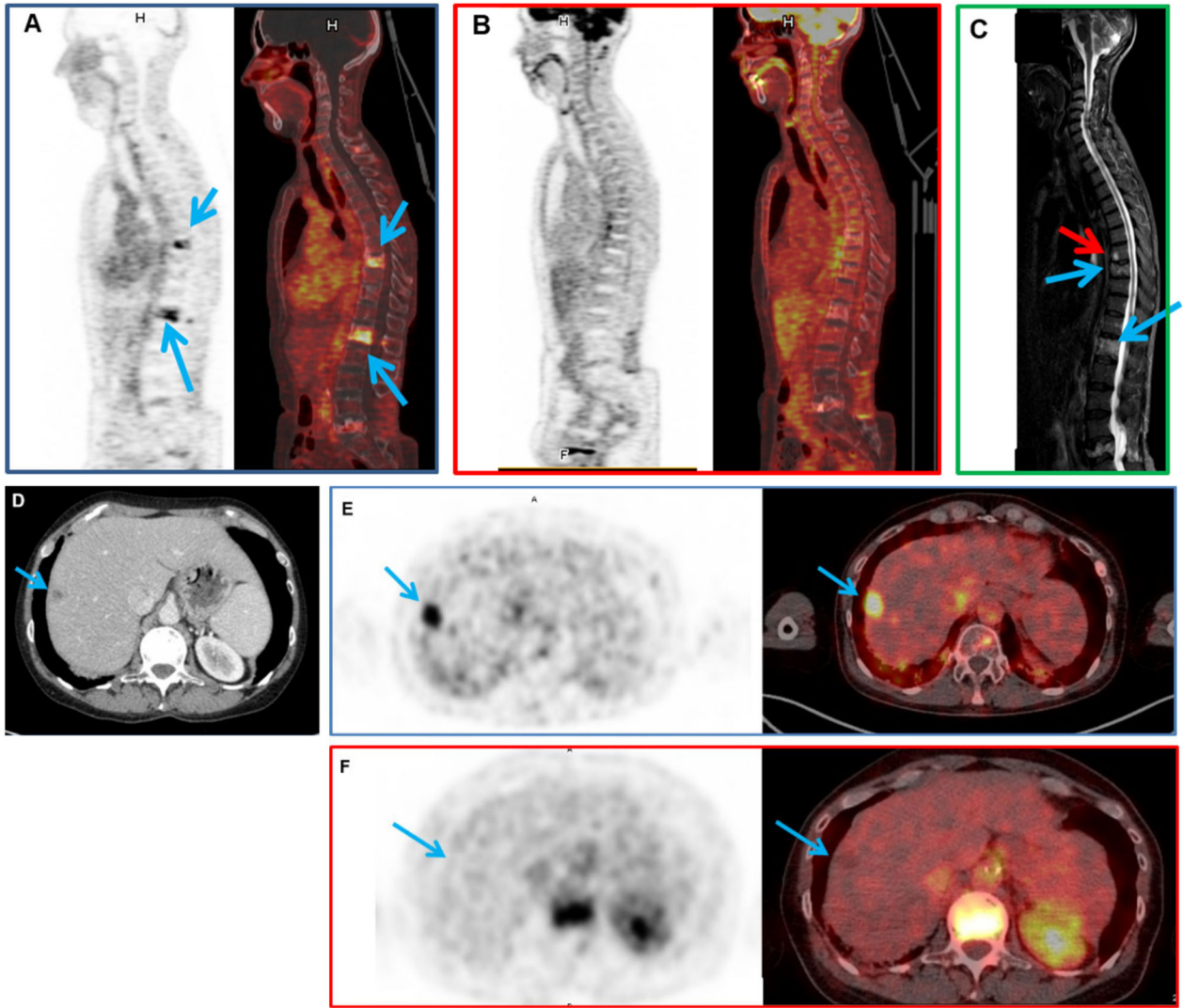


Figure 2: Patient 1. (A) Pretargeted immuno-PET with TF2 and ^{68}Ga -IMP288 peptide images show two vertebral metastases (L1 and T9, blue arrows). (B) FDG-PET discloses no vertebral abnormalities. (C) Vertebral MRI confirmed both lesions and disclosed another at T8 (red arrow). Patient 2. (D) CT shows a suspected liver lesion. (E) Pretargeted immuno-PET with TF2 and ^{68}Ga -IMP288 peptide reveals (blue arrow) a high uptake by a liver lesion not seen by FDG-PET (F).

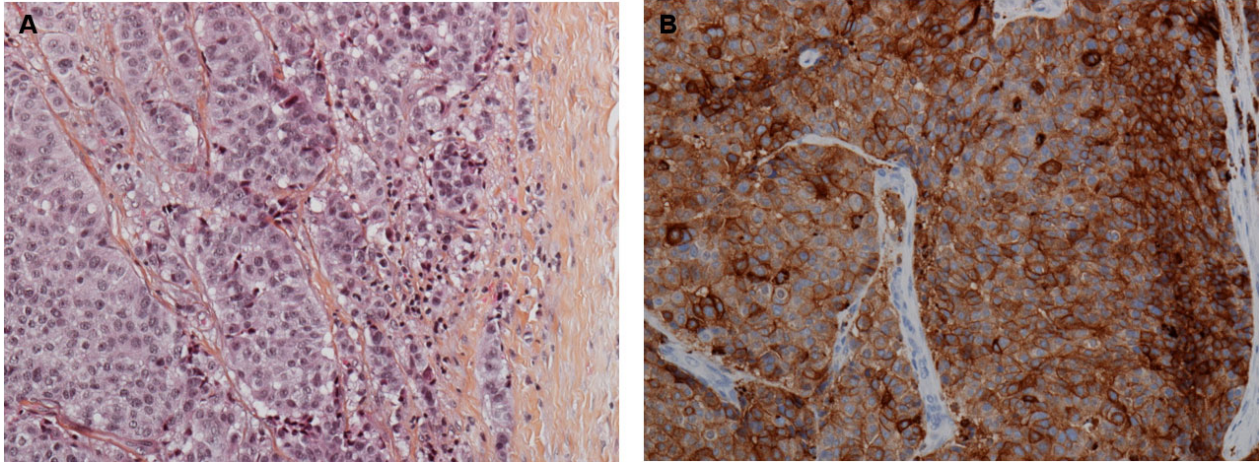


Figure 3: 45 mm left axillary lymphadenopathy excision in a patient with an initial left ductal breast carcinoma, PR 5%, ER 50% and HER2-negative. (A) Carcinoma proliferation surrounded by a fibrous capsule (HES, original magnification x 200). (B) Diffuse and heterogenous (+ to +++) CEA membrane expression in over 50% of carcinoma cells (immunohistochemical study; original magnification x 200).

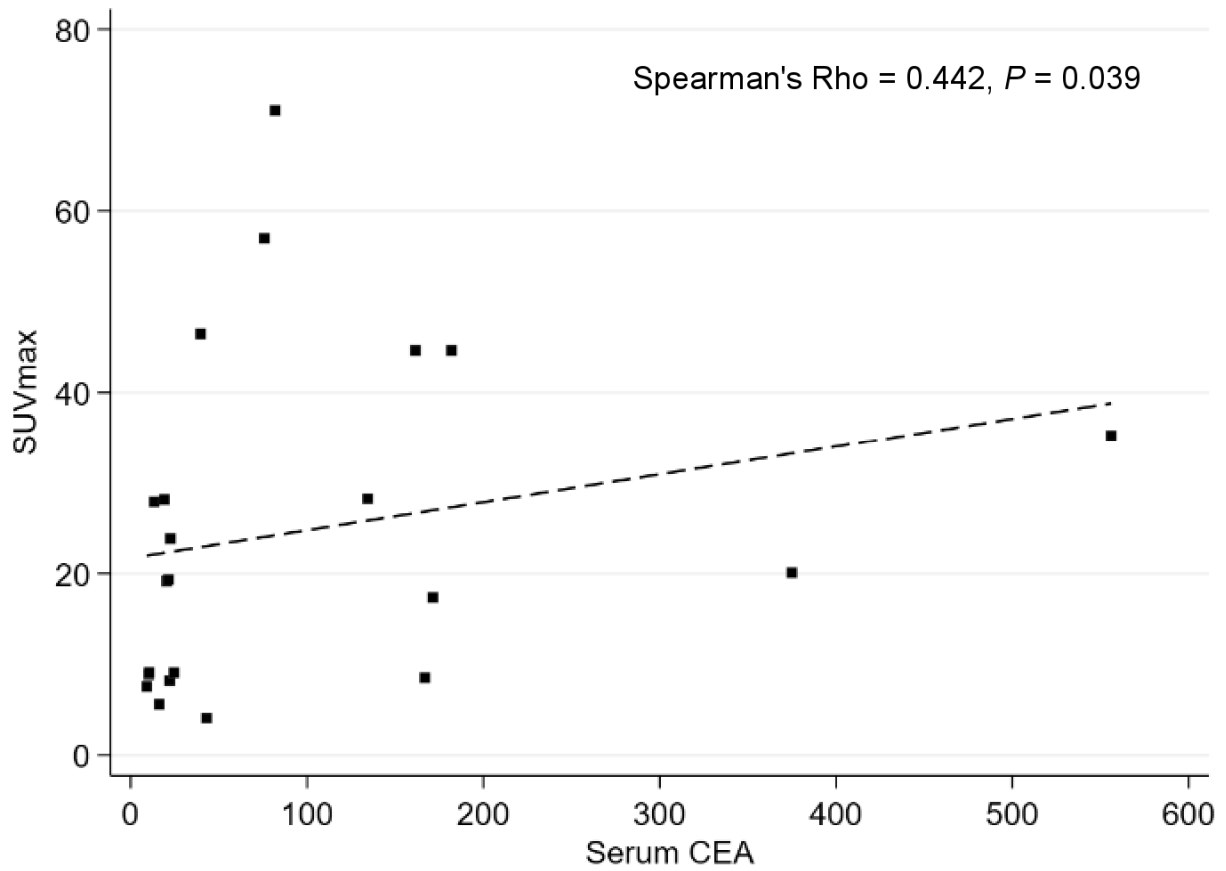


Figure 4 : Correlation between the SUVmax of the most intense lesion in immuno-PET and the serum CEA level (µg/L).

Table 1. Patient characteristics

Total number of patients	23
Median age, years, [range]	61 [37-80]
Initial tumour classification	
T1	7
T2	14
T4	2
Initial Stage UICC	
Stage I	6
Stage IIA	10
Stage IIB	5
Stage IIIB	2
Histology	
Ductal	20
Lobular	3
Hormone Receptor Status	
ER+ and PR+	14
ER+ and PR-	7
ER- and PR+	1
ER- and PR-	1
Histological Grade	
I	1
II	19
III	3
Premenopausal status	2
Postmenopausal status	21
Primary tumour treatment	
<i>Surgery</i>	
Yes	21
No	2
<i>Radiotherapy</i>	
Yes	20
No	3
<i>Adjuvant Chemotherapy (chemo)</i>	
Yes	22
No	1
<i>Adjuvant Hormonotherapy (HT)</i>	
Yes	22
No	1
Number of earlier regimens (chemo, HT)	
1	6
2	1
3	5
>3	11
Median CEA serum level (µg/l), [range]	73.45 [35.1-111.8]
Median Ca15-3 serum level (kU/L), [range]	112.6 [12.4-3,000]
Median CEA Doubling Time, [range]	4.95 mo [0.3-330.1]
Median Ca15-3 Doubling Time, [range]	4.75 mo [0.0-94.1]

ER: Estrogen Receptor; PR: Progesterone Receptor;

Table 2. Sensitivity of immuno-PET, FDG-PET, and conventional imaging.

Location	Immuno-PET	CT	FDG-PET	Axial Bone MRI
Overall	1116 of 1178 (94.7%)	NA	1056 of 1178 (89.6%)	NA
Lymph nodes	61 of 66 (92.4%)	46 of 66 (69.7%)	59 of 66 (89.4%)	NA
Bone	881 of 919 (95.8%)	NA	821 of 919 (89.3%)	412 of 454 (90.7%)
Liver	149 of 153 (97.3%)	141 of 153 (92.1%)	145 of 153 (94.8%)	NA
Lung	14 of 29 (48.3%)	29 of 29 (100%)	22 of 29 (75.9%)	NA

NA: Not Applicable

Table 3. PET semi-quantitative analyses.

	Immuno-PET		FDG-PET		
	median	IQR	median	IQR	<i>P</i> value
Tumor SUV _{max}	23.83	9.09-44.65	15.87	11.70-18.87	0.088
Tumor SUV _{mean}	4.90	3.00-8.16	4.71	3.49-5.62	0.125
Total Tumor Volume	294	159-558	299	139-410	0.256
Total Lesion Activity	2,123	995-5,304	1,197	355-2,433	0.009

SUV: standard uptake value; IQR: interquartile range.